BORE PROPAGATION OVER A SUBMERGED HORIZONTAL PLATE BY PHYSICAL AND NUMERICAL SIMULATION

Daniel B. Bung[1], Arndt Hildebrandt[2], Mario Oertel[1],
Andreas Schlenkhoff[1] and Torsten Schlurmann[2]

An experimental study on the flow patterns around a submerged plate under a propagating bore is presented. Vortices and velocity magnitudes are determined by the PIV method. Parameters are calculated by the open-source code MatPIV and validated by numerical simulations via FLOW-3D with the classical k-ε and the RNG turbulence model on the one hand and a Large Eddy Simulation on the other hand. Furthermore, the influence of the wave period, the wave height and the submersion depth is described.

INTRODUCTION & MOTIVATION

Under the key assumption of linearity, mathematical solutions for progressive small-amplitude water waves provide the basis for solutions of numerous problems. The description and quantification of most phenomena related to coastal and ocean engineering design purposes is made possible. However, some of those essential postulations are unfounded when dealing with water waves being significantly transformed due to interaction with structures. Complex effects like wave breaking, air entrainment or turbulence may become dominant and encourage applying nonlinear models for an appropriate simulation.

Decomposition phenomenon of nonlinear water wave trains passing over a bar or submerged structures, e.g. a positive underwater step, without breaking effects has been investigated experimentally and numerically (Ohyama and Nadaoka, 1994, Ohyama et al., 1994, Beji and Battjes, 1993). In addition, Massel (1983) earlier demonstrates that this phenomenon is triggered by higher harmonic generation and nonlinear resonant interaction over the shelf. Large amounts of energy accumulated in bounded superharmonic components in shallow water regions over the reef are abruptly transferred into freely propagating superharmonic components in the wake of the structure in deeper regions. Since this phenomenon is of great importance for prediction of coastal wave fields and beach profile formation behind the reef, it is also addressed to the variations of the wave spectra during passage over and behind the submerged structure so that the choice of an appropriate analyzing method in time or in frequency domain is important.

---

[1] Hydraulic Engineering and Water Resources Section, University of Wuppertal, Pauluskirchstraße 7, 42285 Wuppertal, Germany
[2] Franzius Institute for Hydraulic, Waterways and Coastal Engineering, University of Hannover, Nienburger Straße 4, 30167 Hannover, Germany

In this regard, Bleck and Oumeraci (2001) perform physical model tests at idealized artificial reefs and principally examine Fourier spectra due to nonlinear transformation processes in front of and behind the submerged structure. Schlurmann et al. (2002) make use of these data to concentrate on the hydrodynamic performance of the artificial reef as a wave height damping structure in coastal regions and, therefore, investigate the incident and transmitted wave spectra derived from time-frequency dependent spectra of monochromatic and irregular waves generated in a laboratory wave flume. They reveal substantial spectral deviations and amplitude variations in time-domain that have neither been revealed by time series analysis methods nor by Fourier analysis techniques.

For a horizontal plate with arbitrary submersion depth, linear analytical solutions of the wave motions are first obtained by Siew and Hurley (1977). In an extension of their work, Patarapanich (1984) studies the maximum and zero reflection caused by the plate. There are numerous further numerical and experimental studies available (see e.g. Ijima et al. 1970, Lengricht et al. 2001 or Liu and Iskandarani 1991).

Recently, Hu and Wang (2005) present a set of analytical solutions for waves propagating past a combined submerged horizontal plate and vertical porous wall breakwater based on linear wave theory velocity potentials. Their analytical solutions in terms of reflection and transmission coefficients as well as the hydrodynamic force on the vertical porous wall are found in good agreement with published laboratory measurements, but fail in case of small relative submersion depths s/d (with s as the submersion depth of the plate and d the water depth) since wave breaking over the plate govern the overall hydraulic performance of the structure in regard to wave damping effects.

The present investigation is aimed at the description of the flow patterns around a submerged plate with small relative submersion depths via physical and numerical simulation.

EXPERIMENTAL SETUPS

Investigations are carried out at two different experimental setups. All PIV measurements are conducted at the University of Wuppertal's Hydraulic Engineering Section. Here a wave with height $H = 4$ cm and period $T = 1$ s is analyzed in a small scale wave flume with a length of 25 m, a width of 0.30 m (Fig. 1). The facility is fully transparent and hence particularly suitable for PIV. The horizontal plate with a length of 50 cm is fixed between the sidewalls to prevent movements of the plate and to eliminate disturbing currents along the longitudinal side of the plate. The distance to the wavemaker is 12.08 m. With the water depth $d = 30$ cm the wave length L can be calculated to 1.37 m and with $s = 6$ cm the relative submersion depth s/d is 0.2.
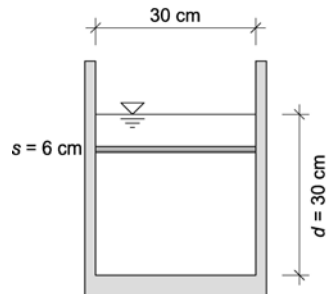
Figure 1. Sectional view of setup 1 for PIV measurements with a fixed relative submersion depths s/d = 0.2 (d = 30 cm).

For better contrast the rear wall is shaded with a black sheet. The required illumination is achieved by three halogen spot lights with 500 W each. Former results gained with this PIV setup are presented in Dätig and Schlurmann (2003) and Harms and Schlurmann (2005).

Further investigations are carried out at the Franzius Institute for Hydraulic, Waterways and Coastal Engineering, University of Hannover, in a 100 m long wave flume with a width of 2.20 m and constant water depth of 0.60 m.
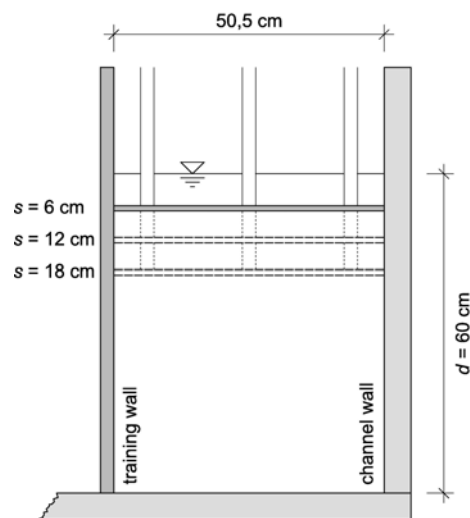
Figure 2.Sectional view of setup 2 for investigation of qualitative flow patterns with varying relative submersion depths s/d = 0.1, 0.2 and 0.3 (d = 60 cm).

Here qualitative flow patterns around the plate are determined with respect of a variation of the submersion depth s, wave period T and wave height H, respectively. For a better illumination of the seeding material, the main channel

width is reduced to 0.505 m by installing a dark training wall. This training wall is 5 m long and extends 2.56 m in front of the plate and 1.64 m behind the plate. Here the horizontal plate mounted in the flume has a length of 0.80 m and is supported by three vertical beams (Fig. 2). For illumination two halogen spot lights with 1500 W each are installed above the flume. The specified setup is positioned 26 m behind the wavemaker where the wave flume consists of a transparent side wall.

Five waves with wave heights H of 5, 10 and 15 cm, wave periods T of 0.96, 1.60 and 2.24 s (and wave lengths L of 1.43, 3.23 and 4.99 m, respectively) are generated to investigate the flow field around the plate (Tab. 1).

Table 1. Generated Waves for investigation of vortex patterns in setup 2.			
	$H = 5$ cm	$H = 10$ cm	$H = 15$ cm
$T = 0.96$ s		x	
$T = 1.60$ s	x	x	x
$T = 2.24$ s		x	

Furthermore three relative submersion depths with $s/d = 0.1$, 0.2 and 0.3 are investigated (Fig. 2). Due to a fixed number of 32 samples per wave period T the measurements are recorded with different sample rates (14.3 Hz for $T = 2.24$ s, 20 Hz for $T = 1.6$ s and 33.3 Hz for $T = 0.96$ s).

NUMERICAL SETUP

A two-dimensional numerical simulation of setup 1 ($d = 30$ cm, $s = 6$ cm, $T = 1$ s, $H = 4$ cm) is conducted for comparison of the flow field around the submerged plate. For this purpose the commercial code FLOW-3D (Version 9.3), which is based on the VOF method, is applied by neglecting surface roughness and hence wall shear stresses. For wave generation the applied version of FLOW-3D offers a special wave boundary condition. Incoming waves are defined by the amplitude, period and phase shift. The specified waves are then assumed to be generated outside of the computational domain as a linear wave. However, once a wave passed the domain's boundary the need for linearity is no more given and non-linear effects are calculated by solving the continuity, momentum and VOF equations. As in the physical model the plate with thickness of 1 cm is mounted at $x = 12.08$ m. The numerical wave flume has a length of 20 m to prevent reflections when rejecting the first unsteady waves and analyzing the following waves. Cell size is 2 cm in length and in height. However, for a better quality of the results in the region of interest (around the plate), cells are refined to 5 mm in both directions. Turbulences are taken into account. Since the expected flow pattern is very complex three different turbulence models are applied for comparison of the

results. Besides a Large Eddy Simulation (LES) and the classical k-ε model the so-called RNG model, which is based on the Renormalization Group method, are applied. The latter approaches are "two equation turbulence models" based on similar equations (Yakhot and Orszag 1986, Yakhot and Smith 1992). However, in RNG model the determination of turbulence parameters as turbulent kinetic energy k and the appropriate dissipation rate ε is achieved by use of statistical methods. While the standard k-ε model implies empirical equation constants, the determination of these constants is explicitly in RNG model. In general, the RNG model offers same applicability as the classical k-ε model. Additionally, the description of flow near walls having strong shear regions is more precise by the RNG model. In LES large scale turbulent flow structures are simulated directly. Small scale eddies have to be approximated by suitable models. Hence, the resolution of the mesh affects the size of resolvable structures.

VELOCITY FIELDS AND VORTEX PATTERNS

PIV measurements

The determination of the velocity fields is carried out by the PIV method in setup 1. Particle Image Velocimetry offers a non-intrusive method to determine the velocity magnitude, the flow direction, the vorticity and the streamlines of water particles within a flow field simultaneously. A seeding material of polyamide spheres with diameters smaller than 1 mm is used for visualization of the flow and all movies are recorded with a high-speed camera (HiSIS 2000) taking 500 frames per second. The open-source code MatPIV v.1.6.1 developed by Sveen (2004) is applied for calculation of flow field characteristics. The frames used for the cross-correlation within the PIV calculation have a time shift $\varDelta t = 0.002$ s. Because of the low resolution of 256 x 256 pixels four separated measurements are performed along the plate in such a manner that each movie shows approximately 20 cm in length and height. However, the subsequent presented results are exemplary concentrated on the trailing edge since a more intensive vortex formation and hence higher energy dissipation is observed here (Fischer 1990).

Fig. 3 presents the results of the PIV investigations for one period with a time step of T/6. The time t is related to the wave period T where $t/T = 0.00$ is defined at the point of the time where the backward directed flow above the plate just sets in. Note that there is an area around the submerged plate which is free of results due to reflections of light occurring above and below the plate.
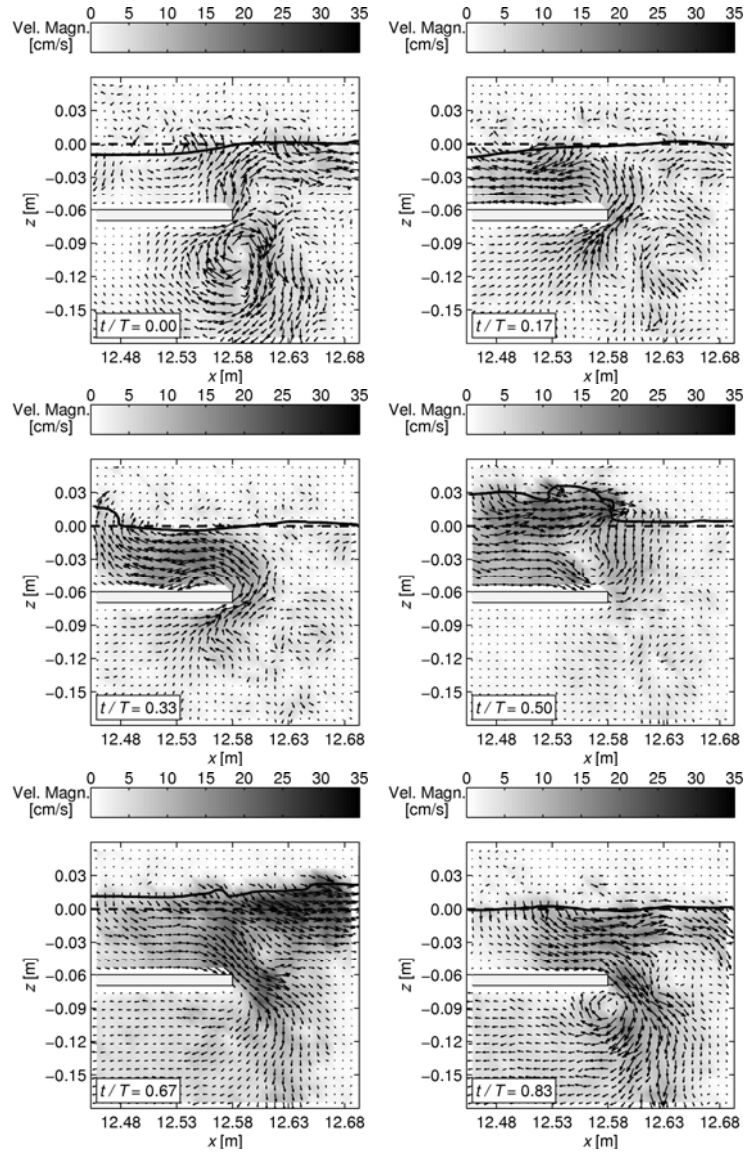
Figure 3. Flow field visualization at different relative points of time t/T from PIV measurement for T = 1.0 s, H = 4 cm and s/d = 0.2 (note that a small region around the plate is free of results due to reflections by the illumination).

By definition, at time $t/T = 0.00$ the water body above the plate is stagnant. Below the rear end of the plate a vortex generated at time $t/T = -0.17$ (or $t/T = 0.83$ respectively) is still visible. However, the whole field is characterized

by low velocities. At $t/T = 0.17$ and $t/T = 0.33$ the flow during the flow reversal under the wave trough is presented. The formation of a large vortex above the plate sets in at its trailing edge by withdrawing water from below. The current velocity for the vortex supply averages 15 cm/s and becomes more intensive with values higher than 20 cm/s directly before the wave breaking. When the wave approaches, the water body above the plate follows the wave propagation direction and the large vortex is closed. The flow field under the breaking wave ($t/T = 0.50$) is characterized by jets with velocities exceeding 30 cm/s. Plunging water mass encounters the relatively calm water body behind the plate and splits up in a major horizontal direction and a minor downwards directed part, which initiates the formation of the vortex at $t/T = 0.83$ and at $t/T = 0.00$ as described earlier. At t/T = 0.67 nearly the whole flow field is in motion. The developing vortex is enforced by the following flow reversal of the wave trough, which sets in and leads to an oscillating current under the plate.

Qualitative analysis of vortex patterns with varying parameters

In the following, exemplary vortex patterns observed in setup 2 are presented. While Fig. 4 includes a variation of the relative submersion depth s/d from 0.1 to 0.3 for $H = 5$ cm and $T = 1.60$ s, vortices for the same wave period but a fixed relative submersion depth of 0.3 and varying wave heights H of 5, 10 and 15 cm are shown in Fig. 5. Values in brackets give the relative point of time t/T where flow phenomena are visible. Again the definition of $t = 0.00$ s is set to where the flow reversal above the plate just sets in.

The relative submersion depth has significant influence on the position of wave breaking for a given wave specified by H and T. The deeper the plate the later wave breaking occurs if any wave breaking provided (Fig. 4). For a given relative submersion depth s/d and wave period T the breaking process sets in earlier with increasing wave height H (Fig. 5). This has direct influence on the vortex pattern and thus affects the currents under the plate, which should be taken into account for sediment and scour estimations.

All investigated wave heights and wave periods show an initial generation of a large vortex shortly after the flow reversal of the wave. This vortex develops counterclockwise during the reversing current at the trailing edge of the plate and gains intensity until the wave breaks and the vortex supplying water from under the plate is interrupted,. Generally, the developing time of this vortex is approximately 34-38 % of the wave period for all configurations. The current caused by the above-mentioned spreading of the flow generates a new vortex or vortex pair, respectively, after $t/T \approx 0.38$. For small values of submersion depth, $s/d = 0.1$, the vortex is dragged to the surface, whereas a downward movement is observed for the relative depth s/d greater or equal to 0.2. The downward directed path of the vortex relates to the wave breaking near the trailing edge of the plate, which induces an impulsive force by the flow of the plunging water mass.

Fig. 4 and 5 point out that the upper vortex becomes more intense with increasing wave height H and submersion depth s. For $H = 5$ cm and $s = 6$ cm a

vortex diameter of 5 cm is generated, while a vortex diameter of 12 cm is found for $H = 10$ cm and $s = 18$ cm. This is related to the increasing wave kinematics, which is orbital velocity and acceleration, with growing wave heights. Moreover, the results indicate that the intensity of the vortex is larger for increasing wave period.
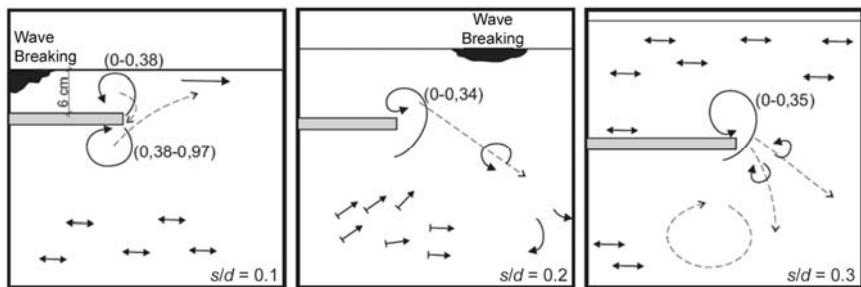

Figure 4. Vortex pattern for relative submerging depth s/d = 0.1, 0.2 and 0.3 (d = 60 cm), wave height H = 5 cm and wave period T = 1.60 s (values in brackets specify the relative time step t/T where t = 0.00 s is set to where the reversal flow above the plate sets in).
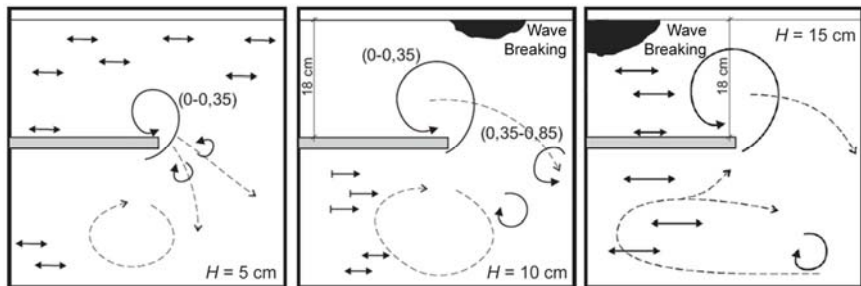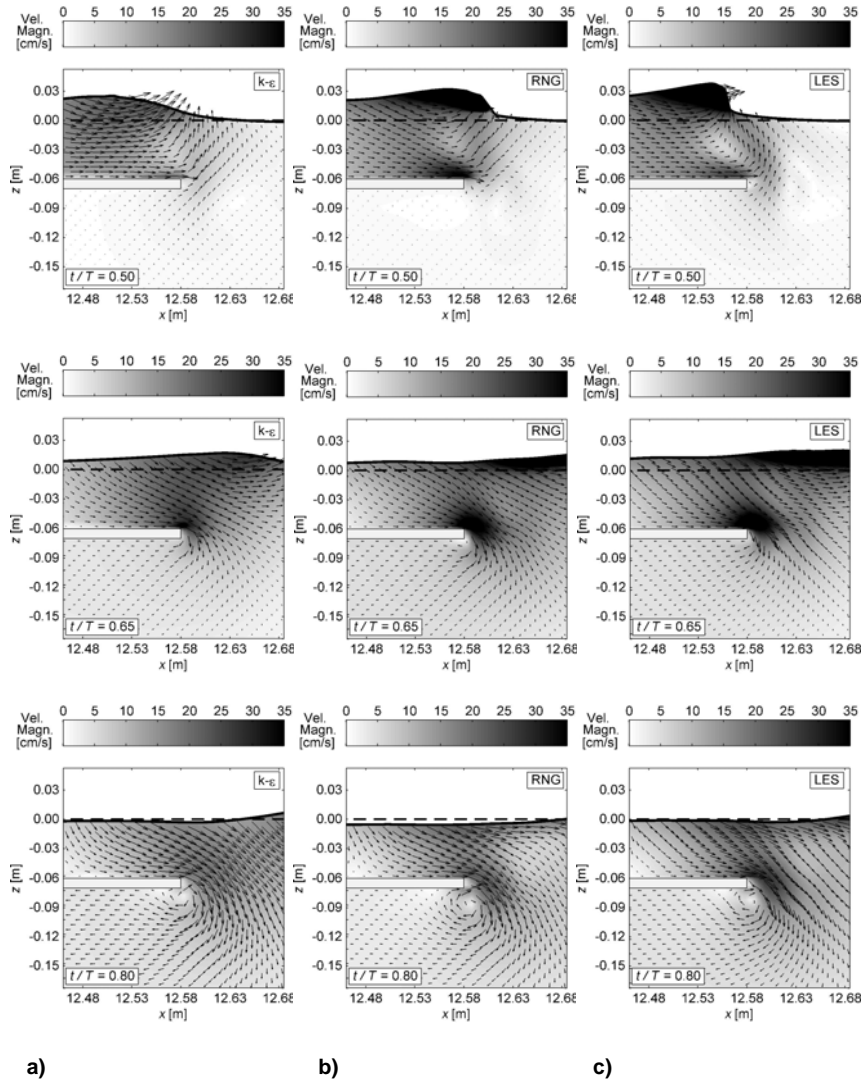

Figure 5. Vortex pattern for relative submerging depth s/d = 0.3 (d = 60 cm), wave period T = 1.60 s and wave heights H = 5, 10 and 15 cm (values in brackets specify the relative time step t/T where t = 0.00 s is set to where the reversal flow above the plate sets in).

RESULTS OF NUMERICAL SIMULATIONS

Fig. 6 presents resulting velocity magnitudes and the flow directions of the numerical simulation for setup 1 at time steps comparable to Fig. 3. The results show good agreement between the physical and the numerical determination of the velocity magnitude. Furthermore, the generation of the characteristic vortices is well represented by all turbulence simulation methods as well as the location and shape of the free surface.

Figure 6 (1). Simulated flow fields at different relative points of time *t*/*T* with (a) k-ε turbulence model, (b) RNG turbulence model and (c) LES turbulence model for *T* = 1.0 s, *H* = 4 cm and *s*/*d* = 0.2.

Figure 6 (2). Simulated flow fields at different relative points of time *t*/*T* with (a) k-ε turbulence model, (b) RNG turbulence model and (c) LES turbulence model for *T* = 1.0 s, *H* = 4 cm and *s*/*d* = 0.2.

However, the resolution of these vortices and hence the quality of the simulation vary. In time step $t/T = 0.00$ the vortex generated earlier is dying out. Here the PIV results indicate a high intensity, which is not obtained by k-ε modeling but by the RNG and LES model. Additionally, the detachment of this eddy (shown in Fig. 3 for $t/T = 0.17$) and the simultaneous high velocity flow at

the trailing edge of the plate are better described by RNG and LES modeling. At $t/T = 0.30$ the reversal flow above the plate is well simulated by all models. A larger and more realistic velocity magnitude is achieved by RNG and LES modeling. Admittedly, it comes along with higher velocity below the plate which is not the case in PIV measurements and hence computed more accurately by the k-ε model. At $t/T = 0.50$ and $t/T = 0.65$ the essential process is given by the spreading of the flow above the plate. Here PIV results in Fig. 3 indicate a high intensity of the jets and an uplift flow in front of the incoming wave while wave breaking begins. All phenomena are represented by LES modeling with high accuracy. On the contrary, it is conspicuous that the wave breaking process and the resulting formation of the jets is not attained by the k-ε model. Indeed, RNG modeling describes both, wave breaking and the plunging jets, but the accuracy achieved by LES simulation is missing.

Generally, if choosing turbulence modeling, the RNG model provides better results than the classical k-ε model. Switching to LES simulation leads to even more accurate results. Although it appeared that calculation time is about 50 % longer when choosing k-ε modeling. Here the calculation time was approximately 1,000 s and 900s for LES and RNG model and 1,500 s for k-ε model (Core Duo PC with 3.06 GHz CPU and 3 GB RAM, MS Windows XP).

CONCLUSION

PIV method is used for the visualization of the flow field behind a submerged plate under a propagating bore. It is demonstrated that vortex formation processes depend on hydraulic boundary conditions as wave period and wave height besides geometric boundary conditions as the relative submersion depth. The different vortex patterns for varying parameters and for different locations on the plate will probably lead to varying loads on the plate. Since earliest wave breaking occurs on the plate, it is assumed that larger loads are affected on its rear end. An analysis will be part of further investigations.

Numerical calculations are conducted with use of different turbulence models. Generally, velocity magnitudes are calculated with adequate precision by all models. However, vortex formation is represented in differing accuracy. Direct simulation of the vortices by LES yields to better results describing the processes in more detail. Comparing the k-ε and RNG turbulence models, both so-called "two equation turbulence models", the RNG model, attaining an accuracy comparable to LES, is preferable.

REFERENCES
Beji, S., and J.A. Battjes. 1993. Experimental investigation of wave propagation over a bar. *Coastal Engineering,* 19, 151-162.
Bleck, M., and H. Oumeraci. 2001, Wave dampening and spectral evolution at artificial reefs, *Proceedings of the International Symposium on Ocean Wave Measurement and Analysis (WAVES 2001)*, ASCE, 2, 1062-1071.

12

Dätig, M., and T. Schlurmann. 2003. Visualization of deep-water breaking waves using a high-speed camera. *Proceedings of the 6th International Conference on Coastal and Port Engineering in Developing Countries (COPEDEC2003)*.

Fischer, C. 1990. Scherschichtdissipation im Nachlauf einer getauchten horizontalen Platte unter dem Einfluss von Oberflächenwellen (Shear layer dissipation behind a submerged horizontal plate under the influence of surface waves). *Hydraulic Engineering Section, University of Wuppertal*, Report No. 15.

Harms, J., and T. Schlurmann. 2005. Time-variant net-mass transport beneath breaking waves, *Proceedings of the 29th International Conference on Coastal Engineering (ICCE2004)*, ASCE, 1, 441-453.

Hu, H., and K.-H. Wang. 2005. Damping effect on waves propagating past a submerged horizontal plate and a vertical porous wall. *Journal of Engineering Mechanics*, 4, 427-437.

Ijima, T., S. Ozaki, Y. Eguchi, and A. Kobayashi. 1970. Breakwater and quay wall by horizontal plates. *Proceedings of the 28th International Conference on Coastal Engineering*, ASCE, 1537-1556.

Lengricht, J., S. Schimmels, T. Schlurmann, and K.-U. Graw. 2001. Whole field velocity mapping in waves. *Proceedings of the International Conference on Ocean Engineering (ICOE2001)*, 2: Marine Hydrodynamics, 95-102.

Liu, P.L.-F., and M. Iskandarani. 1991. Scattering of short-wave groups by submerged horizontal plate, *Journal of Waterway, Port, Coastal and Ocean Engineering*, ASCE, 117, 235-246.

Massel, S. R. 1983. Harmonic generation by waves propagating over a submerged step. *Coastal Engineering*, 7, 357-380.

Ohyama, T. and K. Nadaoka. 1994. Transformation of a nonlinear wave train passing over a submerged shelf without breaking. *Coastal Engineering*, 24, 1-22.

Ohyama, T., S. Beji, K. Nadaoka, and J.A. Battjes. 1994. Experimental verification of numerical model for nonlinear wave evolutions. *Journal of Waterway, Port, Coastal and Ocean Engineering*, 120, 637-644.

Patarapanich, M. 1984. Maximum and zero reflection from submerged plate. *Journal of Waterway, Port, Coastal and Ocean Engineering*, 110, 171-181.

Schlurmann, T., M. Bleck, and H. Oumeraci. 2002. Wave transformation at artificial reefs described by the Hilbert-Huang transformation. *Proceedings of the 28th International Conference on Coastal Engineering*, 2, 1791-1803.

Siew, P.F., and D.G. Hurley. 1977. Long surface wave incident on a submerged horizontal plate. *Journal of Fluid Mechanics*, 83, 141-151.

Sveen, J.K., and E.A. Cowen. 2004. Quantitative imaging techniques and their application to wavy flows. *In: Advances in Coastal and Ocean Engineering, 9, PIV and water waves*, World Scientific, 1-50.

Sveen, J.K. 2004. An introduction to MatPIV v.1.6.1, *Department of Mathematics, Mechanics and applied Mathematics, University of Oslo.*

Yakhot, V., and S.A. Orszag. 1986. Renormalization group analysis of turbulence. I. Basic theory, *Journal of Scientific Computing*, 1, 3-51.

Yakhot, V., and L.M. Smith. 1992. The renormalization group, the ε-expansion and derivation of turbulence models, *Journal of Scientific Computing*, 7, 35-61.